Struct Multidisc Optim (2015) 52:563–582
DOI 10.1007/s00158-015-1263-7

RESEARCH PAPER

3D level-set topology optimization: a machining feature-based approach

Jikai Liu[1] · **Y. -S. Ma**[1]

Received: 4 September 2014 / Revised: 27 March 2015 / Accepted: 30 April 2015 / Published online: 21 May 2015

Abstract This paper presents an explicit feature-based level-set topology optimization method involving polyline-arc profiling and 2.5D machining processes. This method relies on a feature fitting algorithm incorporated into the boundary evolvement process in order to regulate the noisy velocity fields and thus introduce new explicit feature primitives; once inserted, the feature-based shape optimization algorithm is implemented to determine the optimum part shape and topology. The research novelty lies in that, the best-fit feature primitives are inserted during the topology optimization process while other researchers so far have reported only manipulating some existing features with the conventional level-set methods. Therefore, feature-based design can be realized without special requirement of initial input or any post-processing. From the perspective of potential applications, the engineering information embedded in those feature primitives can be extracted and integrated into the optimization formulation. Such potential integration can make the topology optimization even more useful and practical. This effort is an extension of level-set topology optimization into a domain of structural optimization for manufacturing (OFM).

Keywords Level-set topology optimization · Feature fitting · Machining features · Optimization-for-manufacturing

✉ Y. -S. Ma
yongsheng.ma@ualberta.ca

[1] Department of Mechanical Engineering, University of Alberta, Edmonton, AB, Canada

1 Introduction

Topology optimization, as an innovative and optimal part design method, has gained extensive development in the past two decades (Rozvany 2009; van Dijk et al. 2013). The advantage of topology optimization is that it produces optimal conceptual material distribution without initial guess (van Dijk et al. 2013). However, poor regularity of the outcome has been a problem which hinders topology optimization from being integrated into CAD systems. To overcome the problem, a post-treatment step is needed to transform the topologically optimized result into a parametric CAD model for density-based method (Hsu and Hsu 2005; Koguchi and Kikuchi 2006), while parametric approaches like radial basis functions (RBF) (Wang and Wang 2006; Wang et al. 2007; Luo et al. 2008b; Luo et al. 2009; Ho et al. 2011; Ho et al. 2013; Liu et al. 2014) and spline curves/surfaces (Chen et al. 2007; Chen et al. 2008a) are employed for geometry representation by level-set method. This work is based on a parameterized level-set topology optimization method. The objective of this research is to integrate more advanced downstream engineering objects, such as manufacturing feature, into the topology optimization cycles.

Currently, there are mainly two feature-based approaches of level-set topology optimization – the explicit feature-based and implicit feature-based ones. Before introducing the details, a clear definition about ‘explicit’ and ‘implicit’ features should be discussed to avoid confusion. An explicit feature in this context means that the shape feature is parametrically constrained and the shape parameters defined can be used as optimization variables. An implicit feature means the shape of the geometry is approximated without scalable constraints and no shape control parameters are available for further optimization. With regards to the current explicit feature-based approach (Chen et al. 2007; Chen et al. 2008a; Zhou and Wang

2013; Liu et al. 2014), the research efforts mainly maintain and manipulate the existing feature primitives (see Fig. 1a and b). However, there was no mechanism of creating new feature primitives during the topology optimization process. The only relevant work reported was to make the insertion by applying the topological derivative (Cheng et al. 2006; Mei et al. 2008; Gopalakrishnan and Suresh 2008), but that method was not extended into a generic 3D scheme. As for the implicit feature-based approach (Chen et al. 2008b; Luo et al. 2008a; Guo et al. 2014; Allaire et al. 2014), their goals were to approximately satisfy some geometric constraints, like constraining the component thickness within certain maximum and minimum values. However, the lack of explicit feature primitives normally leads to a redundant and manual post-processing step.

This paper focuses on a new explicit feature-based approach which enables fitting explicit feature primitives during the optimization process. With this new method, the level-set topology optimization is free from any initial guess, and can produce explicit feature-based results (as shown in Fig. 1c). It is also worth noticing that, the scale of the resulted feature primitives is controllable which is of great significance in engineering practice.

Another contribution of this paper is that, manufacturing methods are considered upfront with their machining features, i.e., polyline-arc profiles, prismatic 2.5D and freeform 2.5D features. The significance of doing so is that the current 3D topology optimization can only produce approximated freeform design; such constraint severely limits the part design quality, i.e., manufacturability. Normally freeform surfaces warrant 5-axis CNC machining, which requires high-end machine and incurs high costs (So et al. 2007), and long computation and machining times (Lasemi et al. 2010; Masmiati et al. 2012). Comparatively, 2.5D features only require 2.5/3-axis machining, which is more economical and efficient as it uses less costly machine tools, cutters and clamping devices (Verma and Rajotia 2008), and requires significantly less time for code generation and rough-to-finish machining (Masmiati et al. 2012; Xu et al. 2013). Therefore, it will be of great significance for the topology optimization capable of producing 2.5D machining feature-based design.

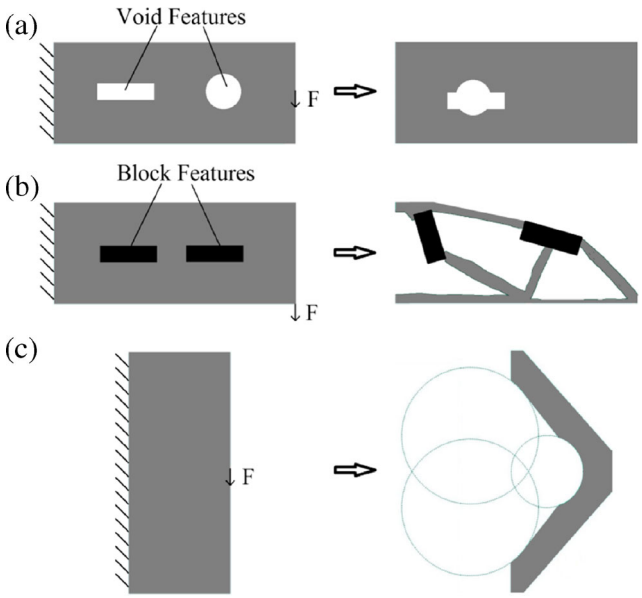

Fig. 1 Results of different explicit feature-based approaches (**a**) conventional explicit feature-based approach (Chen et al. 2007); (**b**) conventional explicit feature-based approach with free boundary evolvement (Kang and Wang 2013; Xia et al. 2013); (**c**) the new explicit feature-based approach developed in this work

Further, design-for-manufacturing (DFM) is a feature-based conceptual design approach which improves the product competitiveness by conducting design activities considering both functional requirements and manufacturing constraints simultaneously (Kerbrat et al. 2011). In this way, the required cutting methods, tools, suggested tolerances, surface finish specifications, and estimated manufacturing cost can be determined in the early design stage (Hoque et al. 2013). Therefore, the introduction of 2.5D machining features into topology optimization algorithm is very useful for integrating manufacturability evaluations into topology optimization. For instance, manufacturing time and cost can potentially work together with mechanical requirements like stiffness and strength, to form the objective function and constraints of the optimization formulation (Fig. 2). This can form a new scheme of optimization-for-manufacturing (OFM).

This paper is organized as follows: Section 2 reviews the development of feature-based level-set topology optimization methods and further explores the manufacturing-oriented considerations. Section 3 introduces the conventional level-set topology optimization method in more details based on the compliance minimization problem. Section 4 describes the working principles of the newly proposed machining feature fitting algorithm involving multiple machining processes. In Section 5, the feature-based shape optimization is introduced to further adjust the constructive feature model. The complete numerical implementation procedures of this novel machining feature-based level-set topology optimization method are summarized in Section 6. Several case studies are given in Section 7 to demonstrate the effectiveness. Section 8 concludes this paper and proposes the future work.

2 Review of literature

2.1 Feature-based level-set topology optimization

Level-set topology optimization (Osher and Sethian 1988; Sethian and Wiegmann 2000; Wang et al. 2003; Allaire et al. 2004), as a popular and powerful structural design method, has attracted great attention in the past decade (van Dijk et al. 2013). A significant advantage of level-set topology optimization is that it allows clear boundary representation. And by

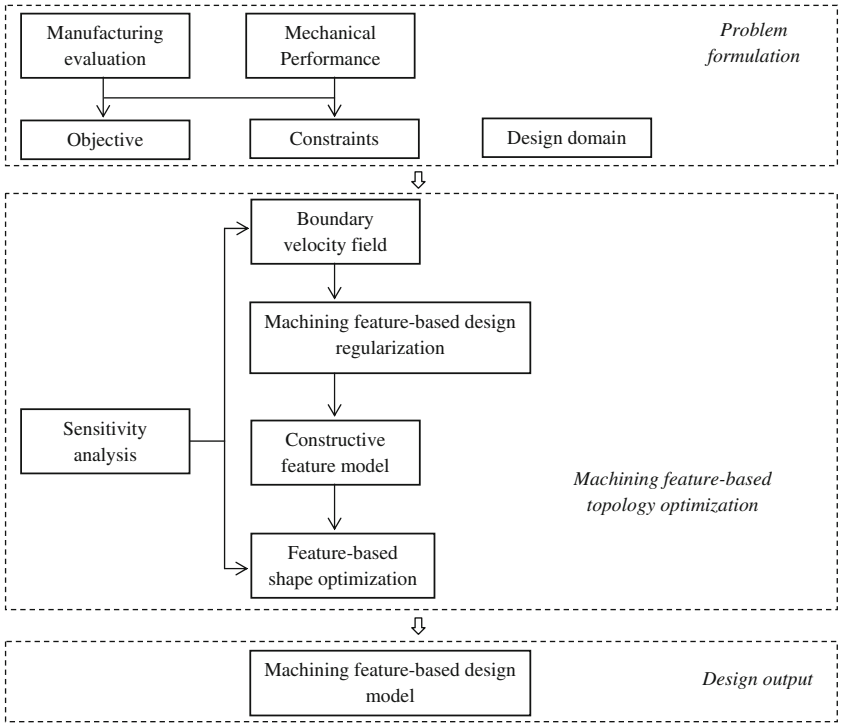

Fig. 2 Conceptual framework of OFM

using parametric level-set functions, the integration with CAD has become possible although manual model mapping is still required.

One group of parametric level-set functions is radial basis functions of different forms and orders that have been applied in level-set topology optimization. It enhances the design space flexibility and convergence speed of the conventional level-set approaches because that new holes can be naturally produced, and the upwind schemes, velocity field, and re-initialization can be eliminated (Wang and Wang 2006; Wang et al. 2007; Luo et al. 2008b; Luo et al. 2009; Ho et al. 2011; Ho et al. 2013; Liu et al. 2014). Alternatively spline curves/surfaces are also commonly used for parameterization (Chen et al. 2007; Chen et al. 2008a).

In recent years, research efforts started to deal with level-set topology optimization with engineering features, because parameterization is not enough for engineering application, yet the featurized geometric shapes with declarative and well-defined form of engineering knowledge need to be addressed (Ma 2013). So far, two streams of feature-based level-set methods have been developed based on shape and topological sensitivity analysis.

The first stream is about implicit feature control. Chen et al. (2008b) and Luo et al. (2008a) applied the quadratic energy functional as part of the objective function and proposed the shape feature control method which successfully realized the strip-like design with controlled thickness. Guo et al. (2014) realized strip-like design by imposing maximum and minimum thickness constraints on the signed distance function. However, simultaneously introducing the maximum and minimum length scale control frequently leads to local optima. Allaire et al. (2014) explored the thickness control mechanism in depth, with diversified schemes of maximum thickness only, minimum thickness only and also the combined manners; additionally, a comparative discussion between thickness control constraints and functionals was demonstrated. In summary, the works under this stream are controlling the shape features in an approximated manner, which is meaningful for cases where the initial feature input is unknown, but the implicit feature-based result is desired.

The second stream is about direct manipulation of the explicit feature primitives. Chen et al. (2007; 2008a) fully parameterized the design domain by implicitly representing the regular shape features with intuitive parameters and the freeform shape features with B-spline; then, the entire model was constructively formed with shape feature primitives through R-functions. The parametric sensitivity analysis and design update are enabled by the differential properties of implicit functions (Shapiro and Tsukanov 1999). Cheng et al. (2006) and Mei et al. (2008) applied a similar method to perform parametric sensitivity analysis on the regular shape feature primitives. More importantly, they developed an initial procedure to topologically introduce explicit feature primitives into the design domain. Zhou and Wang (2013) regulated velocity fields of shape features via least squares fitting to reserve the sharp characteristics; by doing so, they accomplished the explicit feature control with free boundary evolvement simultaneously. More recently, Liu et al. (2014) applied the R-functions to construct the design domain with intuitive-parameter based regular shape features and RBF-based freeform shape features; they inherited the sensitivity

analysis theory for R-functions from (Chen et al. 2007; Chen et al. 2008a), and achieved a unified parametric optimization scheme. Except for the pure level-set approaches, there are also integrated methods which simultaneously optimize the layout of explicit features represented by the level-set function, and the material distribution of supporting structures through density-based method (Kang and Wang 2013; Xia et al. 2013). For these works, efforts are focused on maintaining and manipulating the existing explicit feature primitives, but it is still infeasible to insert new primitives during the optimization process, which is also the case for software tools like PareTO (2013). The only exception is the work from (Cheng et al. 2006; Mei et al. 2008). They applied the topological derivative to insert new explicit feature primitives during the first few iterations of the optimization process. However, as mentioned in the introduction, this method is still not well-developed for several reasons:

- The topological derivative theory is designed to insert infinitesimal holes, but local analysis about the exact feature type to be inserted can be rather sophisticated. Therefore, they developed an in-between feature primitive to be inserted which would approach to the specific feature type during the optimization process. However, they also mentioned that this process was slow (Mei et al. 2008);
- The scale control is far from ideal for the infinitesimal nature of topological derivative. A large number of small in-between feature primitives are inserted at the initial iterations, which generate numerous parameters to be controlled. Furthermore, the final result is composed of too many small segments; a "feature match process" is indispensable to idealize the optimized model, for which the resulting relaxation of the objective value was not discussed;
- This method has not been proven to be effective in 3D scheme.

Gopalakrishnan and Suresh (2008) contributed the feature-specific topological derivative algorithm including both internal and boundary features under 2D scheme. This work provides a preferable theoretical basis for topological sensitivity analysis on inserting certain shape features. However, the possibility and effectiveness of its application in level-set topology optimization has not been explored yet.

At the end of this sub-section, we conclude that a comprehensive explicit feature-based level-set topology optimization method is still in great need. Specifically, this method should have the following characteristics:

- New explicit feature primitives can be automatically selected and inserted during the optimization process;
- The scale of feature primitives should be controllable;
- No post-processing is needed to produce a perfect explicit feature-based design for being directly imported into the CAD system;
- It can be applied for 3D scheme.

All these desired characteristics will be satisfied by the proposed method in this paper, while a comprehensive summary of the performance of existing methods on the listed characteristics above is demonstrated in Table 1.

2.2 Manufacturing-oriented topology optimization

Previously, there were efforts for both the density-based and level-set topology optimization to improve the result manufacturability, covering diversified manufacturing methods like milling and casting (Zuo et al. 2006; Gersborg and Andreasen 2011; Guest and Zhu 2012; Lu and Chen 2012; Xia et al. 2010; Allaire et al. 2013). However, these efforts put more focus on making the result manufacturable but fail to explicitly involve the manufacturing features. Consequently, it is difficult for manufacturability to be quantitatively evaluated; and the manufacturing cost is still relatively high because of the nature of free evolvement. So far, optimization involving manufacturing evaluations like time and cost are only at the parametric shape optimization level (Chang and Tang 2001; Edke and Chang 2006).

3 Review of level-set topology optimization

3.1 Level-set function

Osher and Sethian (1988) proposed the level-set function which is a natural way of closed boundary representation. By solving the Hamilton-Jacobean formulation, the boundary can propagate, merge and split, which makes it perfect for shape and topology optimization.

Let $D \in R^n (n=2 \text{ or } 3)$ be the initial design domain, $\Omega \in R^n (n=2 \text{ or } 3)$ represent the area filled with materials and $\partial\Omega$ be the boundary of the material domain. $\Phi(\boldsymbol{X})$: $R^n \longmapsto R$, is the level-set function that,

$$\begin{cases} \Phi(\boldsymbol{X}) > 0, & X \in \Omega / \partial\Omega \\ \Phi(\boldsymbol{X}) = 0, & X \in \partial\Omega \\ \Phi(\boldsymbol{X}) < 0, & X \in D / \Omega \end{cases} \tag{1}$$

To conveniently apply the level-set function into the optimization process, the Heaviside function and Dirac delta function are adopted as,

$$\begin{cases} H(\Phi) = 1, & \Phi \geq 0 \\ H(\Phi) = 0, & \Phi < 0 \end{cases} \tag{2}$$

$$\delta(\Phi) = \frac{\partial H(\Phi)}{\partial \Phi} \tag{3}$$

Table 1 Characteristics of existing feature-based level-set methods

	In-process insertion of feature primitives	Scale control of feature primitives	Need of post-processing for explicit feature-based result	Applied in 3D schemes
Implicit feature-based approaches:				
Chen et al. (2008b); Luo et al. (2008a); Guo et al. (2014);	Yes	Yes	Yes	To be proved
Allaire et al. (2014);	Yes	Yes	Yes	Yes
Explicit feature-based approaches:				
Chen et al. (2007; 2008a)	No	N/A	No	Yes
Cheng et al. (2006) Mei et al. (2008)	Yes	No	Yes	No
Zhou and Wang (2013)	No	N/A	No	Yes
Liu et al. (2014)	No	N/A	No	To be proved
Method proposed in this paper	Yes	Yes	No	Yes

Then,

$$\Omega = \left\{ X \middle| H(\Phi(X)) = 1 \right\} \tag{4}$$

$$\partial\Omega = \left\{ X \middle| \delta(\Phi(X)) > 0 \right\} \tag{5}$$

Normally, the approximated Heaviside and Dirac delta functions are preferred (Wang et al. 2004; Wang and Wang 2005).

By taking derivative of the zero-value level-set function, the Hamilton-Jacobean equation can be produced:

$$\frac{\partial\Phi(X)}{\partial t} = V_n|\nabla\Phi(X)| \tag{6}$$

in which V_n is the boundary propagating speed in direction of n, and $n = -\frac{\nabla\Phi(X)}{|\nabla\Phi(X)|}$. By solving the optimization formulation and getting the solution of V_n, the Hamilton-Jacobean equation can be updated in each iteration and at the same time, the structure boundary evolves.

3.2 Compliance minimization problem

The work in this paper is based on compliance minimization problems, and the methods can be extended to other design issues. The general form of compliance minimization problems is:

$$\begin{aligned} \min \quad & J(u,\Phi) = \int_D Ae(u)e(u)H(\Phi)d\Omega \\ s.t. \quad & a(u,v,\Phi) = l(v,\Phi), \qquad \forall v \in U \\ & V(\Phi) = \int_D H(\Phi)d\Omega \le V_{max} \\ & a(u,v,\Phi) = \int_\Omega Ae(u)e(v)H(\Phi)dx \\ & l(v,\Phi) = \int_D pvH(\Phi)d\Omega + \int_D \tau v\delta(\Phi)|\nabla\Phi|d\Omega \end{aligned} \tag{7}$$

in which $U=\{v \in H^1(\Omega)^d | v=0 \ on \ \Gamma_D\}$ is the space of kinematically admissible displacement field. A is the Hooke's law for the defined isotropic material and e (u) is the strain. p is the body force acting on the design domain and τ is the traction force acting on the structural boundary. V_{max} is the maximum material volume ratio allowed for the design result.

3.3 Computation of velocity field

In order to solve the compliance minimization problem presented in Eq. (7), finite element analysis and sensitivity analysis are performed to derive the virtual velocity field for the boundary evolvement. This gives the velocity field as shown in Eq. (8) and detailed proof can be found in (Wang et al. 2003; Allaire et al. 2004).

$$V_n = -(\lambda - Ae(u)e(u)) \tag{8}$$

where λ is the Lagrange multiplier for the volume constraint.

The velocity field is composed of continuously varying velocities following a disorganized distribution. Therefore, the topology optimization result tends to be rough 3D freeform. In order to smoothen the freeform result into manufacturable design, a post-processing step is conventionally used to manually construct the parametric freeform design according to optimization result. This step is time-consuming and labor intensive, and more severely, it may unacceptably relax the objective function. In contrast, as shown in Table 1, if 2.5D feature-based geometry is preferred, the proposed method does not need this post-processing step. Further, the new algorithm is fully automated, therefore, it warrants better performance in application.

4 Machining feature fitting algorithm

Machining feature is a domain-specific form of the explicit feature concept. The machining feature fitting algorithm

developed in this work is inspired by feature-based model reconstruction in reverse engineering (Thompson et al. 1999; Rabbani and van den Heuvel 2004; Bi and Wang 2010; Wang et al. 2012), for which different methods have been developed to construct the feature-based models from scanned point cloud. Generally, three major components (Fig. 3) – define feature library, make segmentation and solve the feature fitting problem – exist in these methods, and are suitable to be inherited by our proposed fitting algorithm. Specifically, the feature library includes the candidate feature primitives to be fitted in; segmentation is applied for the piecewise property of feature fitting, as mechanical components are normally composed of numerous feature primitives; then, the nonlinear least squares formulation is adopted to solve the segmented feature fitting problems as shown in Eq. (9).

$$min \quad f = \sum_i d(\boldsymbol{p_i}, \boldsymbol{s})^2 \tag{9}$$

where d is the shortest distance from $\mathbf{p_i}$ to the targeted feature surface, and $\mathbf{s}$ is the parameter set which can uniquely determine the feature profile.

In level-set topology optimization, the boundary velocity field following a disorganized distribution is applied for free evolvement, which is similar to the point cloud in reverse engineering. Therefore, the feature fitting algorithm is appropriate for level-set topology optimization, in order to hold back the free boundary evolvement and eventually produce manufacturable designs. In (Zhou and Wang 2013), the authors applied the least squares fitting to regulate velocity field of existing feature primitives, in this way to maintain and manipulate the feature primitives. However, the method proposed in this paper is trying to insert new feature primitives from candidate machining features, for which there are more design freedoms.

In order to guarantee the completeness of this approach and enable its adaptiveness to different machining processes, the feature fitting algorithm has been developed with polyline-arc profile features, prismatic 2.5D and freeform 2.5D features, respectively.

4.1 Polyline-arc profile (PLAP) features

In this paper, PLAP features are involved because 2D topology optimization widely exists in literature. In practice, PLAP features can be regarded as the contour projection of 2.5D machining features, so it is meaningful to investigate the PLAP features under the machining background. To make it different from free evolvement, the freeform profiles represented by spline curves are not considered here.

There are different taxonomies for PLAP machining features (Miao et al. 2002; Kang et al. 2014), in which numerous specific machining features have been defined and a few cases are illustrated in Fig. 4a. However, it would be ineffective to fit the velocity field with the machining features separately. Therefore, two compound features – the compound slot feature and the compound arc feature – have been defined in this work (Fig. 4b), which can evolve into any specific case as shown in Fig. 4a through solving the feature fitting problem. Mathematically, the velocity fields of the compound features can be represented by Eqs. (10–11).

$$V_{slot}(x) = \begin{cases} V_{line_1}(L_1, C_1) = C_1 \quad x \in [0, L_1) \\ V_{slope_1}(L_2) = C_1 + \dfrac{C_2 - C_1}{L_2 - L_1}(x - L_1) \quad x \in [L_1, L_2) \\ V_{line_2}(L_3, C_2) = C_2 \quad x \in [L_2, L_3) \\ V_{slope_2}(L_4) = C_2 + \dfrac{C_3 - C_2}{L_4 - L_3}(x - L_3) \quad x \in [L_3, L_4) \\ V_{line_3}(L_5, C_3) = C_3 \quad x \in [L_4, L_5] \\ \sum_{i=1}^{5} L_i = L \end{cases} \tag{10}$$

$$V_{arc}(x) = \begin{cases} V_{line_1}(C_1) = C_1 \quad x \in [0, \max(0, x_0 - R)] \\ V_{arc1}(x_0, y_0, R) = \max\left(C_1, \sqrt{R^2 - (x - x_0)^2} + y_0\right) \quad x \in (\max(0, x_0 - R), x_0) \\ V_{arc2}(x_0, y_0, R) = \max\left(C_2, \sqrt{R^2 - (x - x_0)^2} + y_0\right) \quad x \in [x_0, \min(x_0 + R, L)) \\ V_{line_2}(C_2) = C_2 \quad x[\min(x_0 + R, L), L] \\ x_0 \in (0, L) \end{cases} \tag{11}$$

In Eqs. (10–11), C_1, C_2 and C_3 are constants representing the piecewise velocity magnitude; (x_0, y_0) and R are the center position and radius of the circle in the circular arc feature; L represents the total length of the linear segment to be fitted.

For boundary segmentation, it is significant because the feature fitting problems are solved on the basis of piecewise boundary segments. Thus, different fitting results would be produced with different scales of segmentation. For

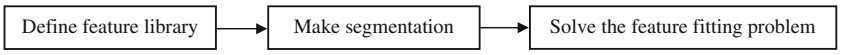

Fig. 3 Three major components of the feature fitting algorithm

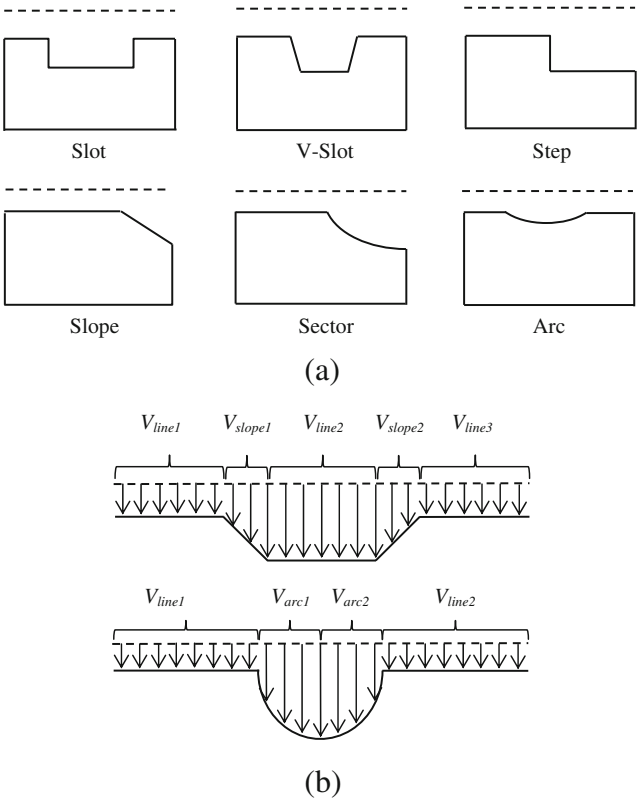

Fig. 4 PLAP machining feature library (**a**) individual features; (**b**) compound features

instance, a linear boundary can be cut into numerous small segments and then each one is fitted with a PLAP feature. In this way, the boundary evolvement can be tracked accurately. However, too many segments are definitely undesirable as they will bring numerous parameters to manage and create difficulties in manufacturing. Therefore, a proper scale of segmentation is significant. In this work, the segments are read from natural boundary definitions; and a customized minimum length scale L_{lim} is employed to filter the small segments out of fitting activities.

As shown in Fig. 5, this algorithm divides the model boundary into 8 linear segments, and the length of each segment is calculated. The following feature fitting problems will only be solved on the segments employing the length larger

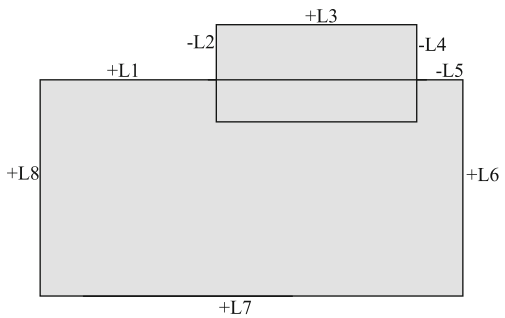

Fig. 5 Boundary segmentation ('+' means the length larger than L_{lim}; '-'means the length shorter than L_{lim})

than L_{lim}, for the purpose of controlling the scale of the newly inserted feature primitives.

After the proper setup of the PLAP feature library and the boundary segmentation, it is designed to apply the least squares formulation as shown in Eq. (12) to regulate the velocity distribution on each piecewise linear segment with the predefined compound feature velocity fields.

$$min \quad f = \int_0^L (V(x,\boldsymbol{s}) - V_n(x))^2 dx \tag{12}$$

Here $V_n(x)$ is the local normal velocity; $V(x,s)$ is the 1D feature velocity as demonstrated in Eqs. (10–11), and s is the optimization variable vector. Given the multiple candidate compound features, the feature fitting problem is finally formulated into a double-layer scheme as,

$$min.\,(min.\,f_i \; by \; finding \; \boldsymbol{s_i})\; i = compound\; slot\; or\; compound\; arc \tag{13}$$

In Eq. (13), the inner loop can be solved by the finite difference method as the analytical expression is hard to derive (Rabbani and van den Heuvel 2004), while the outer loop can be simply solved through comparison.

4.1.1 2.5D features

2.5D machining is a conventional and popular milling method which is greatly preferred by the manufacturing industry for its high efficiency and low cost (Fig. 6). A clear classification of 2.5D machining features is proposed according to (Miao et al. 2002; Kang et al. 2014).

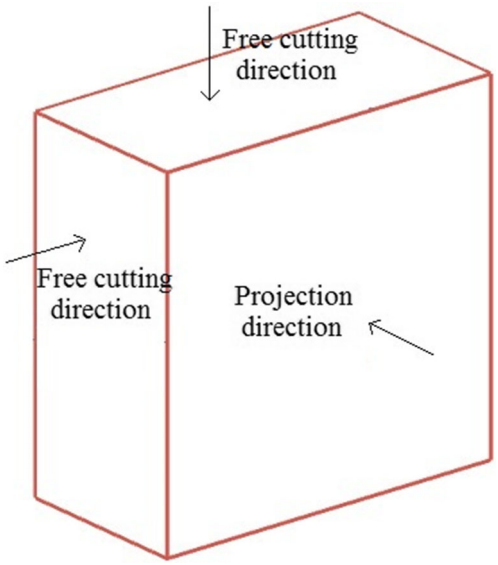

Fig. 6 Directions in the 2.5D milling process

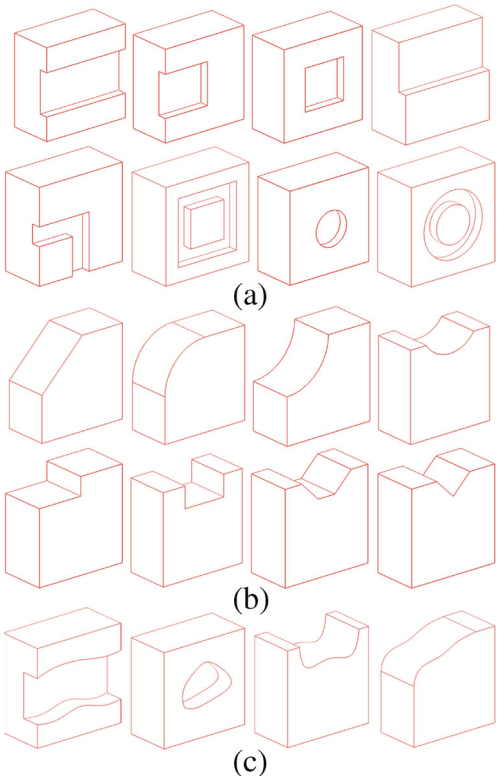

Fig. 7 Classification of 2.5D features (**a**) prismatic 2.5D features in the projection direction; (**b**) prismatic 2.5D features in the free cutting directions; (**c**) freeform 2.5D features

(1) Prismatic 2.5D features

The prismatic 2.5D features employs the contour of general shapes like rectangle and circle, which are the most general 2.5D machining features. Specifically, the prismatic 2.5D features can be divided into two sub-categories, which are fitted in through the projection direction (Fig. 7a) or the free cutting directions (Fig. 7b).

(2) Freeform 2.5D features

The freeform 2.5D features are designed with freeform contours in the cutting directions. It is more complex but still can be handled by the 2.5D machining. Detailed classification of freeform 2.5D features is similar to those demonstrated in Fig. 7a and b, and is shown in Fig. 7c.

Similar segmentation rules as demonstrated in the 2D scheme can be extended to 3D cases, but certain adaptations are needed. Details about the rules will be introduced in the next section because it is tightly connected to the construction method of the feature model.

With regards to the exact 2.5D machining feature fitting algorithm, the least squares formulation demonstrated in Eq. (12) needs to be extended with one more direction as shown in Eq. (14).

$$min \quad f = \int_0^H \left\{ \int_0^L (V(x,y,\boldsymbol{s}) - V_n(x,y))^2 dx \right\} dy \tag{14}$$

The feature fitting problem with prismatic 2.5D features is still a double-layer optimization formulation as shown in Eq. (15), but different feature libraries will be applied for the projection direction and the free cutting directions. Through solving Eq. (15), the best fitted feature and the relevant specifications (size, depth and orientation) for each feasible surface can be found. For instance, a fitting case of the prismatic 2.5D in the projection direction is demonstrated in Fig. 8.

$$min.\ (min.\ f_i\ by\ finding\ \boldsymbol{s_i})\ i = feature\ index \tag{15}$$

As for freeform 2.5D features, the feature fitting problem is adapted into a one-layer optimization problem as shown in

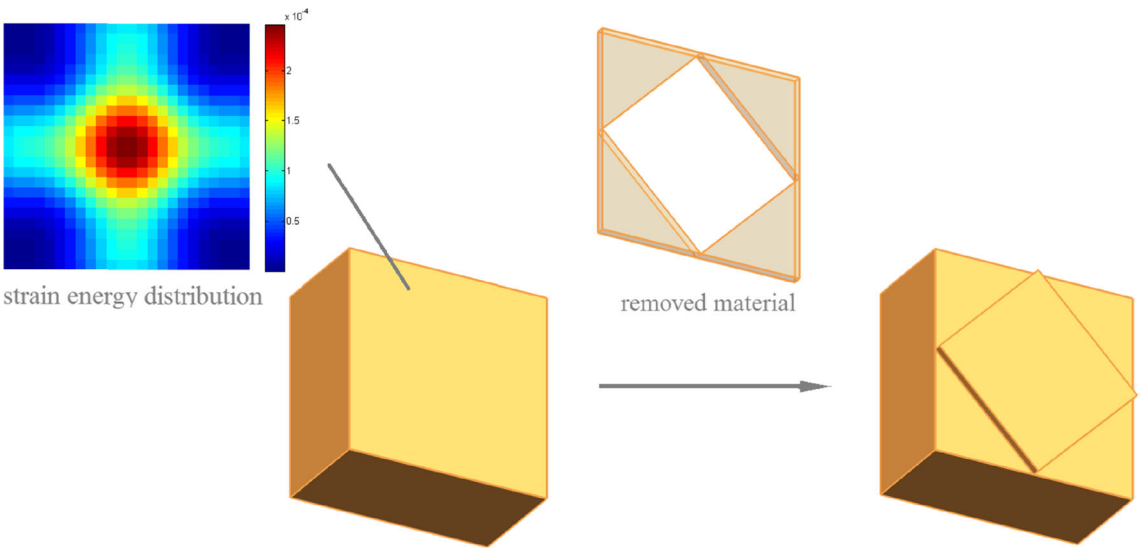

Fig. 8 A fitting case of the prismatic 2.5D in the projection direction

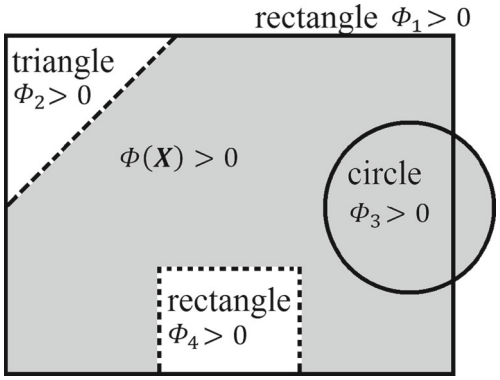

Fig. 9 Constructive feature model

Eq. (16), because of the spline curves applied for the free contour representation.

$$min.\ f\ by\ finding\ \boldsymbol{s}, which\ represents\ the\ set\ of\ control\ points \tag{16}$$

Here, a major problem is to define the projection direction. The strategy applied in this work is to determine the surface employing the highest material removal rate in the initial iteration, and define the relevant normal direction as the projection direction. The reason lies in that the projection direction is normally the major cutting direction.

5 Explicit feature-based shape optimization

Apparently, the material domain after feature fitting is composed of explicit feature primitives, and can be easily transformed into a constructive feature model by R-functions to support the explicit feature-based shape optimization. Further shape adjustments of the material domain can be achieved in a fast and robust iterative manner without relying on the velocity field.

5.1 Constructive model

In CAD systems, constructive and boundary representation are two widely adopted model representation methods, while the latter is more general in commercial software tools. However, for geometric model optimization, sensitivity analysis on the boundary representation requires the model to be isomorphic which severely influence the optimization capability (Chen et al. 2008a). Comparatively, constructive model optimization is insensitive to topology change. Therefore, constructive model is suitable to be the basis of feature-based shape optimization.

To form the constructive model, explicit feature primitives need to be represented in level-set form which describes the volume by point sets. For instance, circle is represented by Eq. (17),

$$\Phi(\boldsymbol{X}) = R - |\boldsymbol{X} - \boldsymbol{X}_0| \tag{17}$$

in which R is the circle radius and $\boldsymbol{X_0}$ is the circle center.

On the other hand, the freeform profiles of the 2.5D features can also be represented implicitly. In this work, the 1-D Bezier curve is applied to represent the freeform profiles for the sake of simplicity (Xu and Ananthasuresh 2003), for which the implicit representation is demonstrated in Eq. (18). Extension to more complex spline curves like B-spline is possible (Chen et al. 2007; Cai et al. 2014).

$$\begin{aligned} \Phi(x,y) &= \left(\sum_{i=0}^{n} B_{n,i}(t(x))Y_i\right) - y \\ B_{n,i}(t) &= \frac{n!}{i!(n-i)!} t^i\ (1-t)^{n-i} \\ t(x) &= \frac{x-K}{L}\ x \in [\,K,\ K+\ L\,] \end{aligned} \tag{18}$$

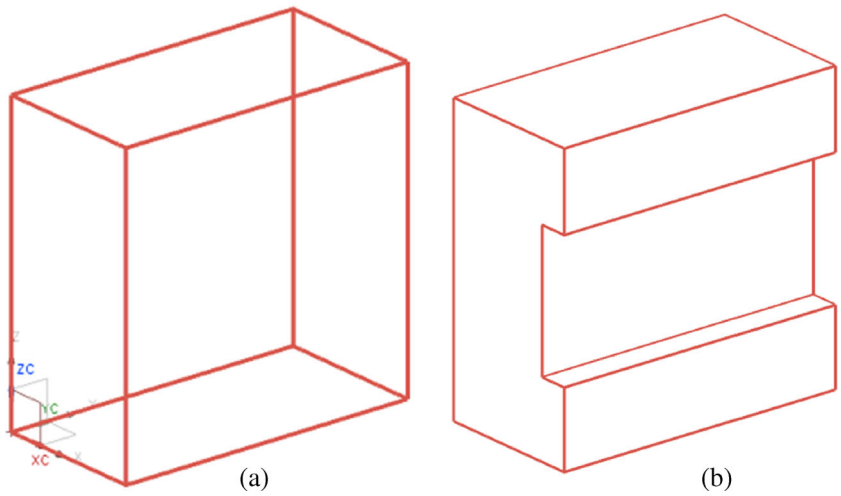

Fig. 10 Boundary segmentation

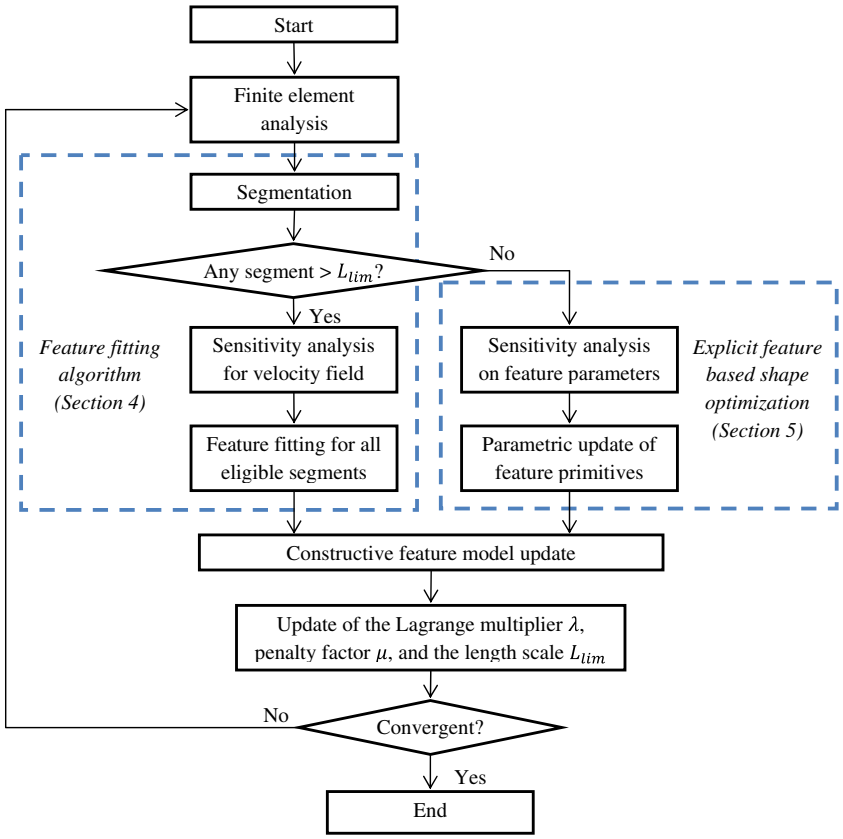

Fig. 11 Flowchart of the implementation procedure

The feature primitives $(\Phi_1(\boldsymbol{X}),\Phi_2(\boldsymbol{X}),\Phi_3(\boldsymbol{X})\ldots\ldots)$ are then combined together by R-functions to form new and complex geometry (Cai et al. 2014),

$$\begin{aligned}\Phi_1\cup\Phi_2 &= \max(\Phi_1,\Phi_2)\\ \Phi_1\cap\Phi_2 &= \min(\Phi_1,\Phi_2)\\ \Phi_1\backslash\Phi_2 &= \min(\Phi_1,-\Phi_2)\end{aligned} \tag{19}$$

In this sense, the integral level-set function will be,

$$\Phi = C(\Phi_1,\Phi_2,\Phi_3,\ldots\ldots) \tag{20}$$

In Fig. 9, the integral level-set function is formed by R-function as $\Phi=(\Phi_1\cup\Phi_3)\backslash(\Phi_2\cup\Phi_4)$.

So far, the constructive feature model has been introduced in details. Therefore, the boundary segmentation rules are presented here for its tight connection with the construction method.

As presented in Fig. 10a, the constructive feature model composed of only one primitive can be represented by:

$$\Phi(\boldsymbol{X}) = \Phi_1(\boldsymbol{X}) = min\left[\frac{L}{2}-(x-x_0),\ \frac{L}{2}+(x-x_0),\frac{W}{2}-(y-y_0),\frac{W}{2}+(y-y_0),\frac{H}{2}-(z-z_0),\frac{H}{2}+(z-z_0)\right] \tag{21}$$

in which L, W, H are the lengths in x, y, z directions, respectively; and (x_0, y_0, z_0) is the coordinate of the center point. Correspondingly, the front boundary segment in x direction is represented by:

$$\left\{\boldsymbol{X}\middle|\frac{L}{2}-(x-x_0)=0\ and\ \Phi(\boldsymbol{X})=0\right\} \tag{22}$$

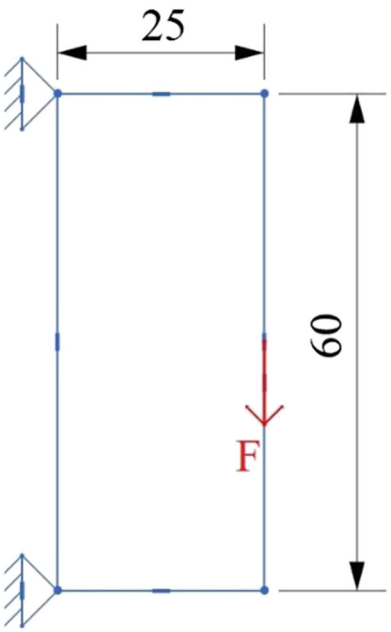

Fig. 12 Short cantilever problem in 2D

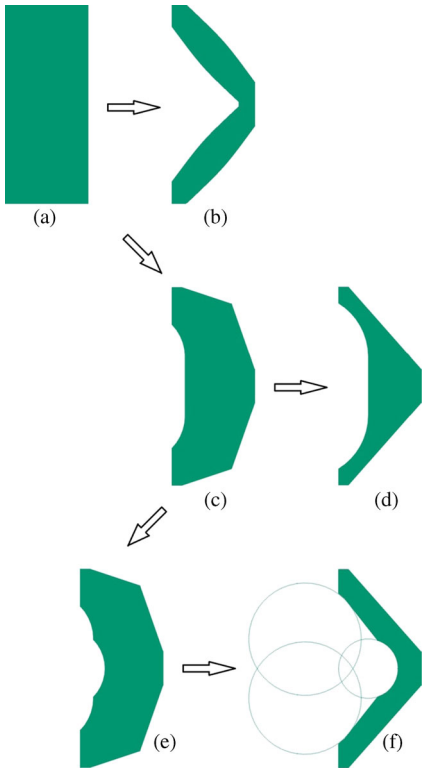

Fig. 13 Optimization processes of different schemes

In Eq. (22), the last term is naturally satisfied, because Φ (X) is identical to Φ_1 (X). However, it is significant to have the Φ (X) = 0 term in this representation, because only the overlapping boundaries between the feature primitive and the constructive feature model will be tracked as effective boundary segment for feature fitting.

If fit in another primitive Φ_2 to the front face in x direction as presented in Fig. 10b, the constructive level-set function will be:

$$\Phi(\boldsymbol{X}) = \Phi_1(\boldsymbol{X}) \Big/ \Phi_2(\boldsymbol{X}) \tag{23}$$

$$\Phi_2(\boldsymbol{X}) = \min\left[\frac{L'}{2} - \left(x - x_0'\right), \frac{L'}{2} + \left(x - x_0'\right), \frac{W'}{2} - \left(y - y_0'\right), \frac{W'}{2} + \left(y - y_0'\right), \frac{H'}{2} - \left(z - z_0'\right), \frac{H'}{2} + \left(z - z_0'\right)\right] \tag{24}$$

Then, the front boundary segment of primitive Φ_1 in x direction is still tracked by Eq. (22), but the effective area has changed. The effective boundary segment of primitive Φ_2 is tracked by Eq. (25).

$$\left\{\boldsymbol{X} \middle| \left[\frac{L'}{2} - \left(x - x_0'\right) = 0 \; or \; \frac{L'}{2} + \left(x - x_0'\right) = 0\right] and \; \Phi(\boldsymbol{X}) = 0\right\} \tag{25}$$

In this way, all effective boundary segments can be accurately tracked during optimization. Another point to be emphasized is that the orientation (projection direction, or one of the free cutting directions) of each created explicit feature primitive should be recorded. For each of the primitive, only boundary segment perpendicular to the recorded orientation will be considered for further feature fitting.

As for size of the boundary segment, it is counted by the number of included mesh points.

5.2 Sensitivity analysis

Because the feature primitives are represented by implicit level-set functions and their shapes are directly decided by the intuitive parameters or control points, the sensitivity

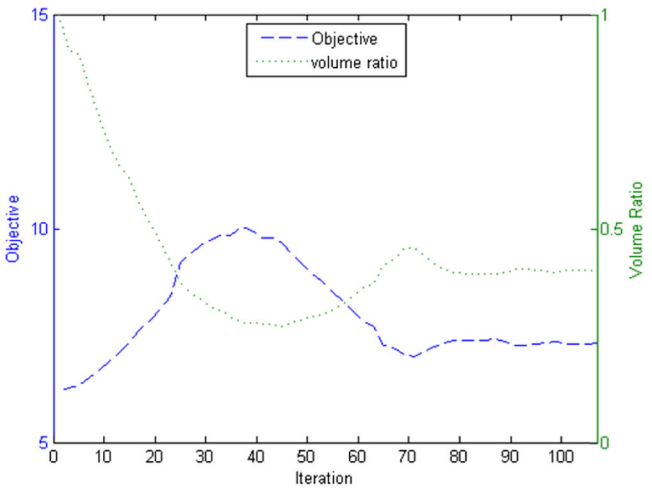

(a)

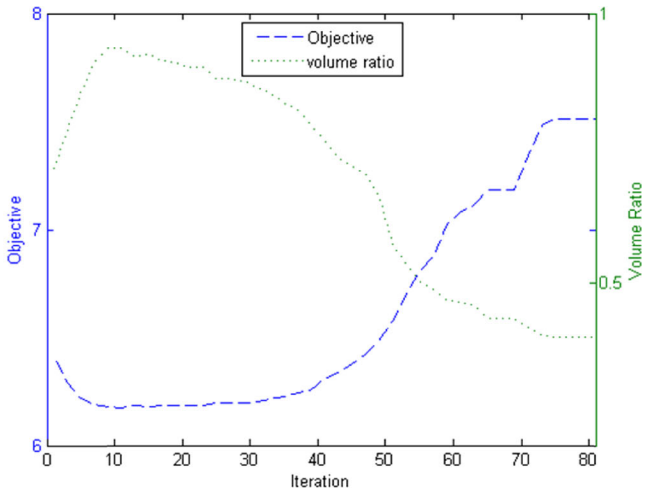

(b)

Fig. 14 Convergence histories (**a**) regular level-set approach; (**b**) machining feature-based approach with customized length scale L_{lim}=15

analysis on the shape parameters or control points can be calculated by applying Eq. (26).

$$\frac{\partial p_j}{\partial t} = -\int_D R \frac{\partial \Phi}{\partial \Phi_i} \frac{\partial \Phi_i}{\partial p_j} \delta(\Phi) d\Omega \tag{26}$$

where p_j means the j^{th} shape parameter (control point) of shape (spline curve) i, and R is called shape gradient density.

$$R = -Ae(u)e(u) + \lambda \tag{27}$$

Details about the proof of Eqs. (26–27) can refer to (Chen et al. 2007).

After sensitivity analysis, design update can be done parametrically Eq. (28) instead of solving the Hamilton-Jacobi Equation for non-parametric shape optimization.

$$p_j = p_j + \frac{\partial p_j}{\partial t} * \Delta t \tag{28}$$

6 Numerical implementation details and procedures

In this work, the finite element analysis (FEA) is implemented on fixed quadrilateral/hexahedral meshes to solve the linear elastic problem as depicted in Eq. (7). The artificial weak material is applied for voids in order to avoid the singularity of the stiffness matrix, as

$$E = 10^{-3} E_m (1 - H(\Phi)) + E_m H(\Phi) \tag{29}$$

in which E_m is the elastic modulus for the solid material.

The volume constraint is satisfied by applying the Augmented Lagrange method which adopts the Lagrange multiplier as,

$$\begin{aligned} \lambda_{k+1} &= \lambda_k + \mu_k \left(\int_D H(\Phi) d\Omega - V_{max} \right) \\ \mu_{k+1} &= \alpha \mu_k \; where \; 0 < \alpha < 1 \end{aligned} \tag{30}$$

With regards to the convergence algorithm, the steepest descent method guarantees the feature fitting and parameter adjustment in the descent direction. Specifically, the velocity field is only involved in a few iterations to fit in new feature primitives; while in most iterations, the parametric shape optimization make the convergence process fast and efficient (Chen et al. 2008a).

As for the feature fitting algorithm, the customized length scale L_{lim} is applied in an increasing manner to save computational expense and to avoid the infinite loop. That is,

$$\begin{aligned} {L_{lim}}^{k+1} &= \beta {L_{lim}}^{k} \\ \beta &\geq 1 \end{aligned} \tag{31}$$

Additionally, a few special filter principles are: first, the feature primitives fitted in with very small magnitudes need to be filtered out; second, ineffective feature primitives will be detected and filtered out for every a few shape optimization iterations, which targets at the feature primitives either not effectively forming part of the model boundary or employing zero-valued sizing parameters.

In summary, all the numerical skills mentioned above guarantee the efficiency comparable or even better compared with existing level-set methods.

In Fig. 11, the complete numerical implementation procedures are demonstrated, and the overall algorithm is illustrated step by step as below:

Table 2 Quantitative comparison between extruded 2.5D result and the conventional 3D level-set result

	Extruded 2.5D result	Conventional 3D level-set result	Rate of increase compared with the conventional 3D result
Compliance (under the volume ratio of 0.3)	8.02	7.88	1.78 %

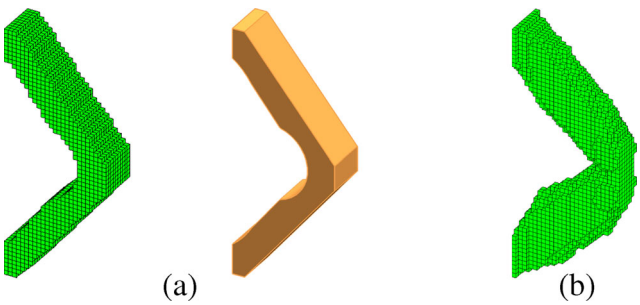

Fig. 15 Comparison between extruded 2.5D result and the conventional 3D level-set result (**a**) gird and iso-contour model of extruded 2.5D result (**b**) grid model of conventional 3D level-set result

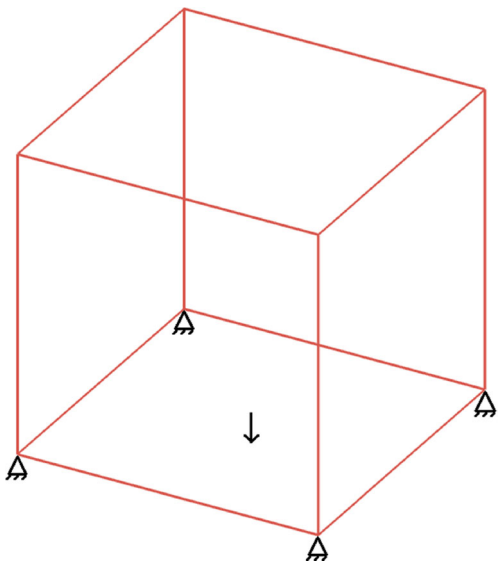

Fig. 16 Cube problem

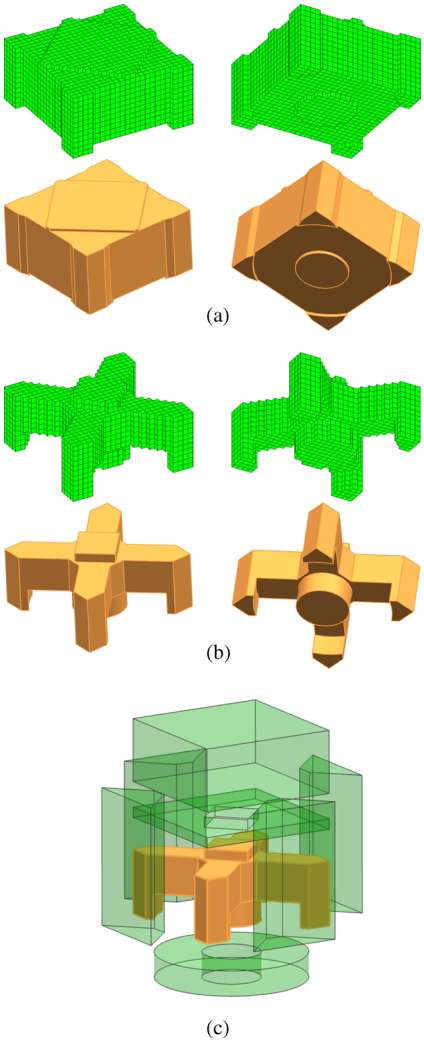

Fig. 17 Results of the machining feature-based approach with L_{lim}= 20*20 (**a**) result after feature fitting; (**b**) final result; (**c**) the final result with removed 2.5D features

Step 1: Initialize the constructive feature model by defining the level set functions and the Boolean operations. Define the projection direction and the free cutting directions. Set the Lagrange multiplier λ, penalty factor μ, and the length scale L_{lim}.

Step 2: Perform finite element analysis to evaluate the deformation field.

Step 3: Make segmentation and measure the segment sizes.

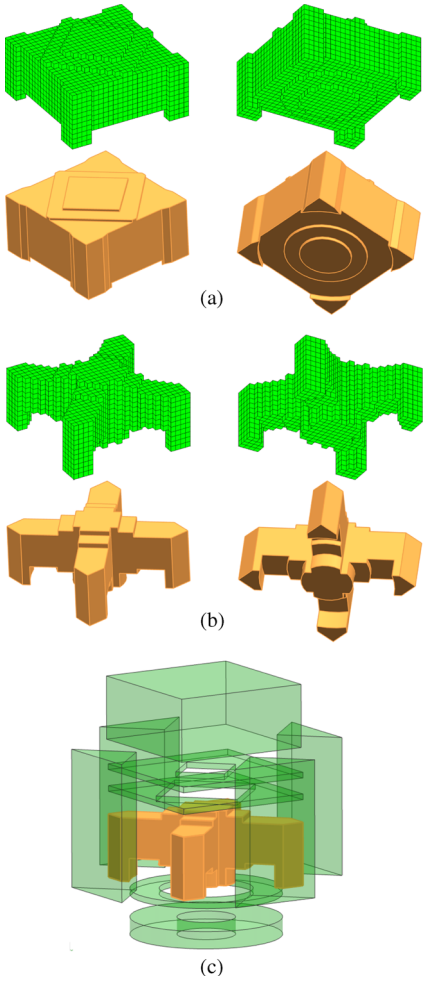

Fig. 18 Results of the machining feature-based approach with L_{lim}= 14*14 (**a**) result after feature fitting; (**b**) final result; (**c**) the final result with removed 2.5D features

Step 4: If there are segments eligible for feature fitting (size $> L_{lim}$), go to Step 4.1; otherwise, go to Step 4.2.

- Step 4.1. Solve the feature fitting problems on all eligible segments to fit in new feature primitives. Go to Step 5.
- Step 4.2. Perform sensitivity analysis on existing feature primitive parameters and update the relevant feature primitives. Go to Step 5.

Fig. 19 Result of conventional 3D level-set approach

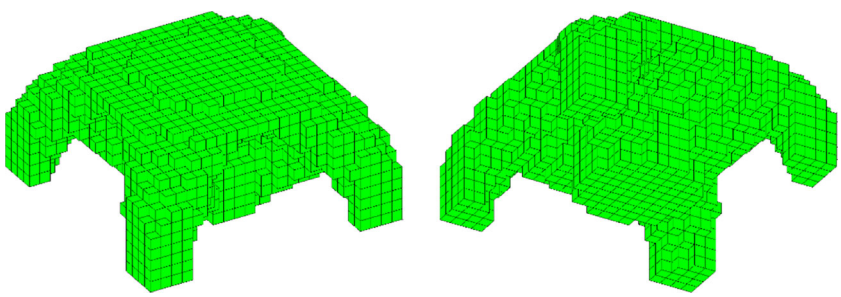

Table 3 Data of the three different results

	Machining feature-based result (L_{lim}=20*20)	Conventional 3D result	Rate of increase compared with the conventional 3D result
Compliance (under the volume ratio of 0.2)	14.58	13.62	7.04 %
	Machining feature-based result (L_{lim}=14*14)	Conventional 3D result	Rate of increase compared with the conventional 3D result
Compliance (under the volume ratio of 0.2)	14.07	13.62	3.30 %

Step 5: Update the constructive feature model with either new feature primitives (if go through Step 4.1) or new parameter values (if go through Step 4.2).

Step 6: Update of the Lagrange multiplier λ, penalty factor μ, and the length scale L_{lim}.

Step 7: Check if the termination condition is satisfied. If yes, then a convergent solution is found; otherwise, go through Step 2 to Step 6.

It should be noticed that if L_{lim} is bigger than the maximum possible boundary segment size, the algorithm will ignore Step 3 and Step 4.1 in order to save computational effort.

7 Case study

7.1 Short cantilever problem – the PLAP case

The first case is about the short cantilever problem as shown in Fig. 12. The top and bottom of the left side are fixed and a vertical unit force pointing downward is loaded at the middle of the right side. The objective is to minimize the compliance with the maximum volume ratio of 0.4. Poisson ratio and Young's modulus are 0.3 and 1 respectively.

To manifest the influence of adding the feature fitting algorithm into the optimization process, the regular level-set approach and the machining feature-based approach with customized length scale L_{lim}=15 have been implemented in this case. Their results and the convergence histories are illustrated in Figs. 13 and 14, respectively.

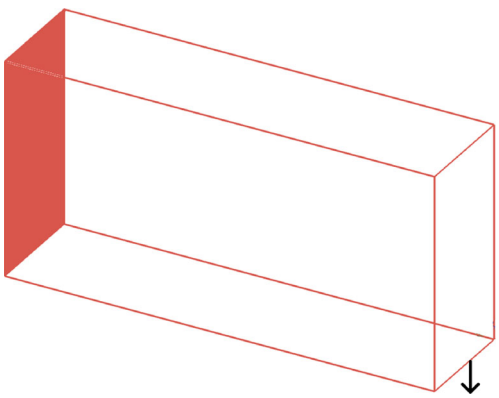

Fig. 20 Cantilever problem in 3D

In analysis of these two optimization processes, the regular level-set approach takes 107 iterations and adapts the design from Fig. 13a to b with the final objective of 7.3101. Then the machining feature-based approach takes 81 iterations, and the design follows the adaption path of (a)-(c)-(e)-(f) in Fig. 13, for which the objective ends at 7.5128. Through comparison of these two results, it can be concluded that the regular level-set approach is able to reach the optimal objective but its design manufacturability is relatively low; while machining feature-based approach can achieve the desired design with great manufacturability, in condition that the objective is not overly sacrificed.

An extra feature-based process with enlarged length scale L_{lim}=25 is tested in this case. This process adapts the design

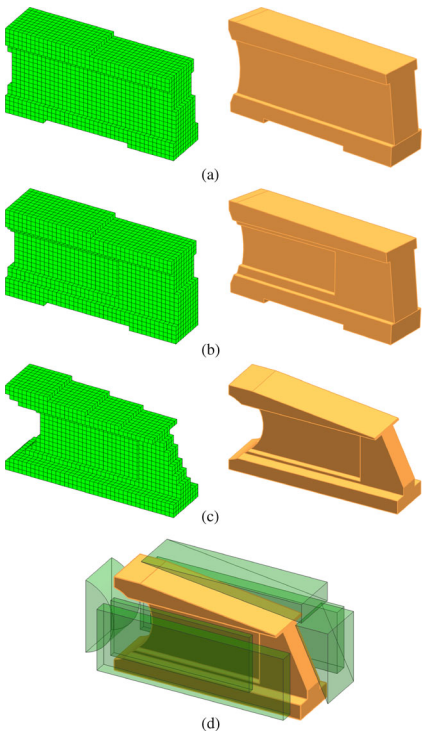

Fig. 21 Optimization process of the prismatic 2.5D machining feature-based approach with L_{lim}=10*20 (**a-b**) intermediate results; (**c**) the final result; (**d**) the final result with removed 2.5D features

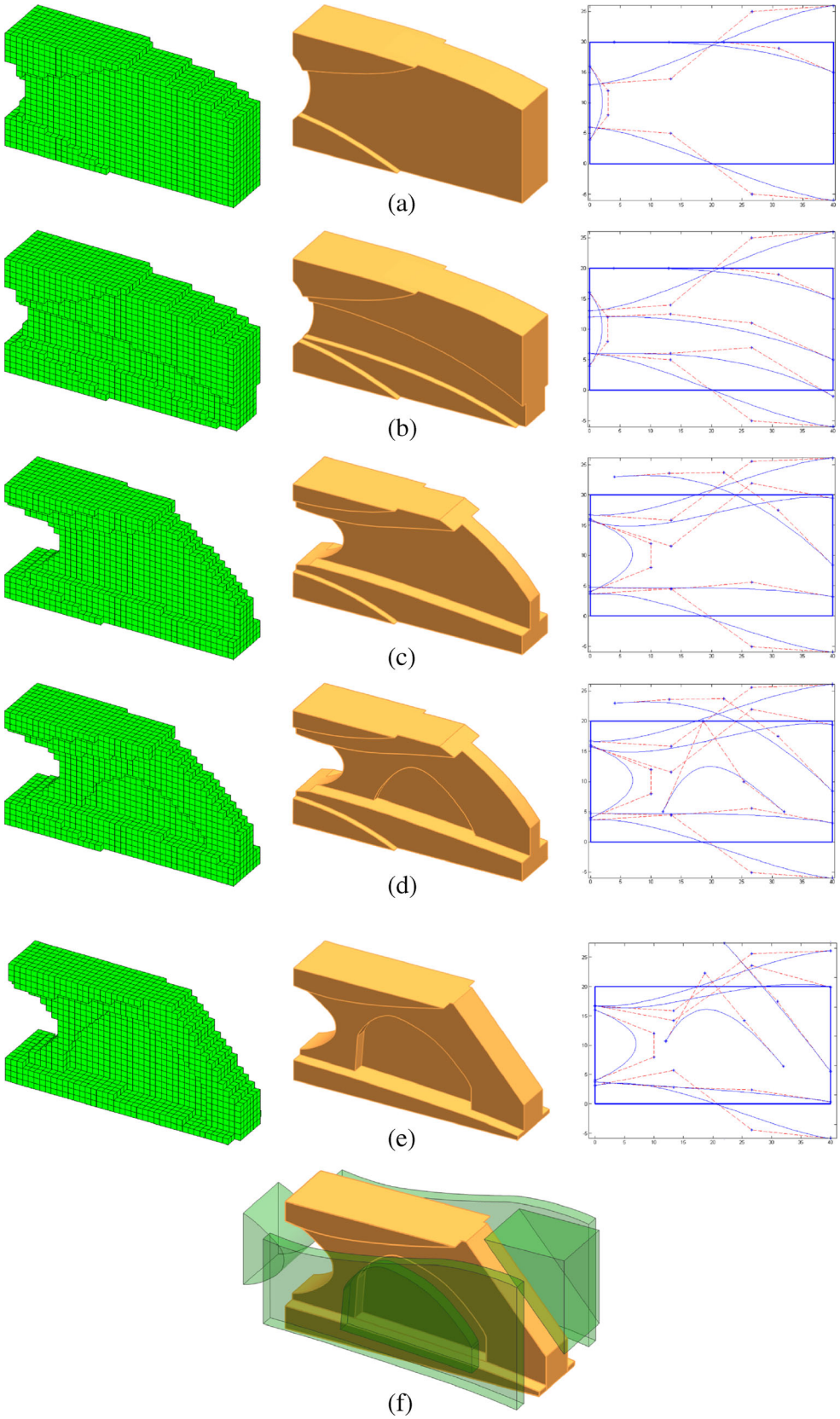

Fig. 22 Optimization process of the freeform 2.5D machining feature-based approach with L_{lim}=10*20 (**a-d**) intermediate results; (**e**) final result; (**f**) the final result with removed 2.5D features

following the path of (a)-(c)-(d) in Fig. 13, and its final compliance is 8.7760 which is 20.29 percent higher than the optimum. Through this test, the significance of appropriately selecting the customized length scale is emphasized.

A similar case appeared earlier in (Mei et al. 2008). Their result consists of many small feature primitives, for lack of scale control capability. Consequently, manufacturability is still problematic unless adopting the post-treatment of boundary smoothing.

(1) regular level-set approach (a-b);
(2) machining feature-based approach with customized length scale L_{lim}=15 (a-c-e-f);
(3) machining feature-based approach with customized length scale L_{lim}=25 (a-c-d)

As mentioned earlier, the 2D features can be regarded as the contour projection of the 2.5D machining features. Therefore, we extrude the 2D design with the depth of 10, and compare it with the conventional 3D level-set result. From Fig. 15 and Table 2, it can be seen that the 2.5D result employs the compliance nearly at the same level with the conventional 3D result, but has much better manufacturability.

7.2 Cube problem

In this case, the design domain (as shown in Fig. 16) is a cube (24*24*24) with its four bottom corners fixed and a force of magnitude 2 loaded at the bottom center. The objective is to minimize the compliance under the volume constraint of 0.2. Poisson ratio and Young's modulus are 0.3 and 1 respectively.

Three different optimization schemes have been adopted to demonstrate the effectiveness of the machining feature-based approach, as well as the scale control ability. The first scheme is the machining feature-based approach with customized length scale L_{lim}=20*20, and the results are shown in Fig. 17. Comparatively, the second scheme is still the machining feature-based approach, but with the customized length scale L_{lim}=14*14, for which the results are illustrated in Fig. 18. Finally, the conventional 3D level-set approach is applied to derive the freeform 3D result as shown in Fig. 19.

Data of the three different results is listed in Table 3. Through data analysis, it can be concluded that the conventional 3D level-set approach can derive the optimum, while the machining feature-based approach slightly sacrifices the optimality in order to improve the desired manufacturability. On the other hand, smaller customized length scale can lead the objective closer to the optimum. In fact, the 3D level-set approach is equivalent to the machining feature-based approach with infinitesimal customized length scale.

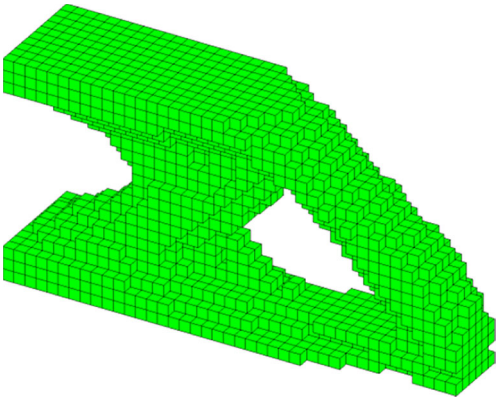

Fig. 23 Result of conventional 3D level-set approach

Practically this may take more time to machine as smaller tools and multiple tool changes may need to be used.

7.3 Cantilever problem

The 3D cantilever (40*10*20) problem is depicted in Fig. 20, where the left side is fixed and a vertical force (magnitude=2) pointing downward is loaded at the middle bottom of the right side. The objective is to minimize the compliance with the maximum volume ratio of 0.4. Poisson ratio and Young's modulus are 0.3 and 1 respectively.

In this case, two different schemes have been defined and will be commented in a comparative manner:

- The first scheme is the machining feature-based approach with prismatic 2.5D features;
- The second scheme is the machining feature-based approach with freeform 2.5D features;

Table 4 Statistic comparison between the machining feature-based and the conventional 3D results

	Prismatic 2.5D result	Conventional 3D result	Rate of increase compared with the conventional 3D result
Compliance (under the same volume ratio of 0.4)	45.49	43.28	5.11 %
	Freeform 2.5D result	Conventional 3D result	Rate of increase compared with the conventional 3D result
Compliance (under the same volume ratio of 0.4)	43.87	43.28	1.36 %

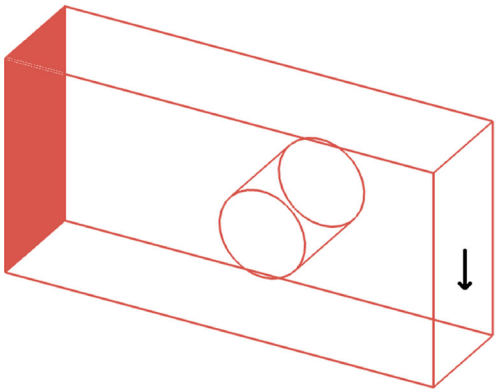

Fig. 24 Cantilever problem with fixed hole

For the first scheme, the results are demonstrated in Fig. 21. In Fig. 21a, two symmetric shallow pockets in the projection direction, and one pocket, two slopes and one arc surface in the free cutting directions are fitted in. Then from (a) to (b), a pair of symmetric pockets is fitted in again in the projection direction. After these feature fitting activities, the feature-based shape optimization converges to 45.49 of compliance and 0.4 of volume ratio.

For the second scheme, the intermediate results are shown in Fig. 22a-d, in which the 3D grid and iso-contour models, as well as the 2D Bezier curves have been demonstrated. Control points of the Bezier curves have been designated as the variables of the feature-based shape optimization. Consequently,

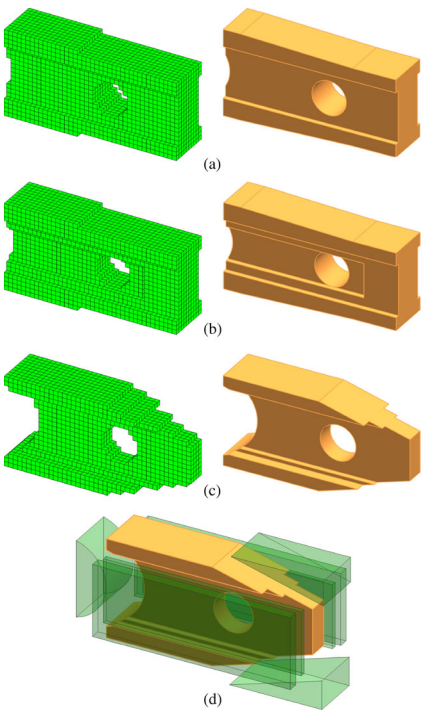

Fig. 25 Optimization process of prismatic 2.5D machining feature-based approach with L_{lim}=10*20 (**a-b**) intermediate results; (**c**) the final result; (**d**) the final result with removed 2.5D features

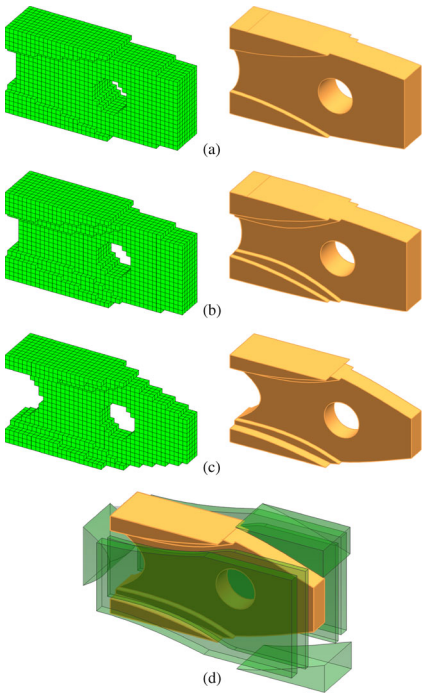

Fig. 26 Optimization process of freeform 2.5D machining feature-based approach with L_{lim}=10*20 (**a-b**) intermediate results; (**c**) the final result; (**d**) the final result with removed 2.5D features

the final result is demonstrated in Fig. 22e, for which the volume ratio is 0.4, and the compliance is 43.87.

To fairly comment the 2.5D machining feature-based approaches, the conventional 3D level-set result is demonstrated in Fig. 23. It is clear that both machining feature-based approaches can derive results with much better manufacturability. Considering more details, the freeform 2.5D result (Fig. 22e) employs the shape and topology much closer to the conventional 3D result, when compared with the prismatic 2.5D result (Fig. 21c). This is owing to the more design freedoms of spline curves compared with regular shape parameters. However, the small sacrificing of the objective of the prismatic 2.5D result brings even better manufacturability, as well as the convenience for the downstream design change management, because prismatic 2.5D features are preferred in commercial modelling systems. Therefore, the choice

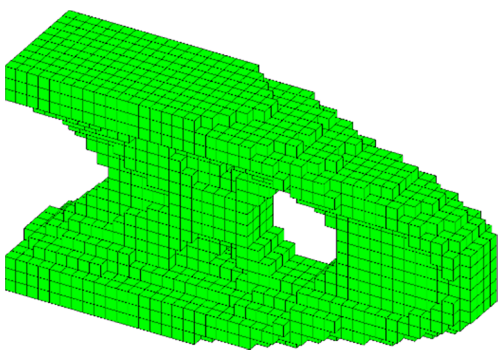

Fig. 27 Conventional 3D level-set result

Table 5 Statistic comparison between the machining feature-based and the conventional 3D results

	Prismatic 2.5D machining feature-based result	Conventional 3D result	Rate of increase compared with the conventional 3D result
Compliance (under the same volume ratio of 0.4)	34.65	33.30	4.05 %
	Freeform 2.5D machining feature-based result	Conventional 3D result	Rate of increase compared with the conventional 3D result
Compliance (under the same volume ratio of 0.4)	33.52	33.30	0.66 %

between freeform and prismatic 2.5D machining feature-based approaches is a trade-off between better objective and the simplicity in further design change management. In Table 4, a set of data analyses is demonstrated.

7.4 Cantilever problem with fixed hole

The 3D cantilever (40*10*20) problem depicted in Fig. 24 employs the same problem initialization with the case demonstrated in Sub-Section 7.3. However, there are two major differences: a fixed hole exists in the design domain for purpose of assembly; and the force is loaded at the middle of the right side wall, which makes the final design vertically symmetric. This is a benchmark case cited from (Zhou and Wang 2013) to better demonstrate the effectiveness of our novel machining feature-based approach.

Figure 25 presents two intermediate results (a-b), as well as the final design (c) of the regular 2.5D machining feature-based approach. Compared with the prismatic 2.5D case presented in Sub-Section 7.2, the optimized result in this case is evidently different in the configuration of feature primitives, and specially, the symmetric design in this case employs better compliance of only 34.65 with volume ratio of 0.4.

As for the freeform 2.5D machining feature-based approach, the intermediate results are shown in Fig. 26a and b, and consequently, the final result is demonstrated in Fig. 26c, for which the volume ratio is 0.4, and the compliance is 33.52.

The conventional 3D level-set result is shown in Fig. 27. Through comparison, it can be concluded that the material distributions are very similar among Figs. 25c, 26c and 27. Therefore, the mechanical performances can be predicted and are close as shown in Table 5. Readers who have interest can refer to (Zhou and Wang 2013) for a similar 3D result.

At the end of the case study section, the computation times of the 2.5D and 3D examples have been summarized in Table 6. All computations are performed by Matlab with Core CPU of 3.3GHz. From the data, it can be concluded the 3D scheme is the most time-consuming, because it has more design freedoms and takes more iterations to converge. For the 2.5D scheme, the feature fitting activities increase the computation time, and sometimes make it close to the 3D scheme. Additionally, the freeform 2.5D scheme takes more iterations to converge than the regular 2.5D.

8 Conclusion

This paper presents a novel machining feature-based level-set topology optimization method, which relies on the feature fitting algorithm and the feature-based shape optimization to derive optimized machining feature-based design. Specially, the feature fitting algorithm applies the least squares fitting to piecewise regulate the disorganized boundary velocity fields, and thus realize the insertion of machining feature primitives; feature-based shape optimization optimizes the constructive feature model resulting from feature fitting to derive the final optimum. Theoretically, this new approach allows more design freedom through conditionally inserting feature primitives during the optimization process, and therefore, fills the gap of only maintaining and manipulating the existing feature primitives of the conventional feature-based level-set methodes.

From the perspective of engineering application, this new method is designated to employ the manufacturing background. Machining features of PLAP, prismatic 2.5D and freeform 2.5D have been applied as the candidate feature primitives. Therefore, manufacturability of the topology

Table 6 Computation times of the 2.5D and 3D examples (seconds)

	Prismatic 2.5D examples	Freeform 2.5D examples	3D examples
The cube problem	866/914	–	1426
The cantilever problem	817	1085	1519
The cantilever problem with fixed hole	761	1012	1098

optimization result is no longer a problem. Additionally, the introduction of machining features makes it possible to integrate the underlying engineering information into the optimization formulation. For instance, evaluations like manufacturing time and cost can be part of the objective and constraints. Therefore, a new concept of OFM is proposed, which is so far only explored to derive the machining feature-based design. How to integrate the manufacturing information into the optimization formulation is still not explored in depth, which will be a major future work.

Besides, this machining feature-based approach can potentially be further developed and extended with even more manufacturing methods and engineering contexts.

Acknowledgments The authors would like to acknowledge the financial support: NSERC Discovery grants, MITACS accelerate cluster internship support, and China Scholarship Council (CSC) student scholarship. All the research works were carried out at University of Alberta.

References

Allaire G, Jouve F, Toader AM (2004) Structural optimization using sensitivity analysis and a level-set method. J Comput Phys 104: 363–393

Allaire G, Jouve F, Michailidis G (2013) Casting constraints in structural optimization via a level-set method. 10th World Congress on Structural and Multidisciplinary Optimization, Orlando, Florida, USA May 19–24

Allaire G, Jouve F, Michailidis G (2014) Thickness control in structural optimization via a level set method. doi: http://hal.archives-ouvertes.fr/hal-00985000

Bi ZM, Wang LH (2010) Advances in 3D data acquisition and processing for industrial applications. Robot Comput Integr Manuf 26:403–413

Cai SY, Zhang WH, Zhu JH, Gao T (2014) Stress constrained shape and topology optimization with fixed mesh: a B-spline finite cell method combined with level set function. Comput Methods Appl Mech Eng 278:361–387

Chang KH, Tang PS (2001) Integration of design and manufacturing for structural shape optimization. Adv Eng Softw 32:555–567

Chen JQ, Shapiro V, Suresh K, Tsukanov I (2007) Shape optimization with topological changes and parametric control. Int J Numer Methods Eng 71:313–346

Chen JQ, Freytag M, Shapiro V (2008a) Shape sensitivity of constructively represented geometric models. Comput Aided Geom Des 25: 470–488

Chen SK, Wang MY, Liu AQ (2008b) Shape feature control in structural topology optimization. Comput Aided Des 40:951–962

Cheng GD, Mei YL, Wang XM (2006) A feature-based structural topology optimization method. IUTAM symposium on topological design optimization of structures. Mach Mater 505–514

Edke MS, Chang KH (2006) Shape optimization of heavy load carrying components for structural performance and manufacturing cost. Struct Multidiscip Optim 31:344–354

Gersborg AR, Andreasen CS (2011) An explicit parameterization for casting constraints in gradient driven topology optimization. Struct Multidiscip Optim 44:875–881

Gopalakrishnan SH, Suresh K (2008) Feature sensitivity: a generalization of topological sensitivity. Finite Elem Anal Des 44:696–704

Guest JK, Zhu M (2012) Casting and milling restrictions in topology optimization via projection-based algorithms. Proceedings of the ASME 2012 International Design Engineering Technical Conference & Computers and Information in Engineering Conference, Chicago, IL, USA, August 12–15

Guo X, Zhang WS, Zhong WL (2014) Explicit feature control in structural topology optimization via level set method. Comput Methods Appl Mech Eng 272:354–378

Ho HS, Lui BFY, Wang MY (2011) Parametric structural optimization with radial basis functions and partition of unity method. Optim Methods Softw 26:533–553

Ho HS, Wang MY, Zhou MD (2013) Parametric structural optimization with dynamic knot RBFs and partition of unity method. Struct Multidiscip Optim 47:353–365

Hoque ASM, Halder PK, Parvez MS, Szecsi T (2013) Integrated manufacturing features and design-for-manufacture guidelines for reducing product cost under CAD/CAM environment. Comput Ind Eng 66:988–1003

Hsu MH, Hsu YL (2005) Interpreting three-dimensional structural topology optimization results. Comput Struct 83:327–337

Kang Z, Wang YQ (2013) Integrated topology optimization with embedded movable holes based on combined description by material density and level sets. Comput Methods Appl Mech Eng 255:1–13

Kang M, Kim G, Eum K, Park MW, Kim JK (2014) A classification of multi-axis features based on manufacturing process. Int J Precis Eng Manuf 15:1255–1263

Kerbrat O, Mognol P, Hascoet JY (2011) A new DFM approach to combine machining and additive manufacturing. Comput Ind 62:684–692

Koguchi A, Kikuchi N (2006) A surface reconstruction algorithm for topology optimization. Eng Comput 22:1–10

Lasemi A, Xue DY, Gu PH (2010) Recent development in CNC machining of freeform surfaces: a state-of-the-art review. Comput Aided Des 42:641–654

Liu T, Wang ST, Li B, Gao L (2014) A level-set-based topology and shape optimization under geometric constraints. Struct Multidiscip Optim. doi:10.1007/s00158-014-1045-7

Lu JN, Chen YH (2012) Manufacturable mechanical part design with constrained topology optimization. Proc Inst Mech Eng B: J Eng Manuf 226:1727–1735

Luo JZ, Luo Z, Chen SK, Tong LY, Wang MY (2008a) A new level set method for systematic design of hinge-free compliant mechanisms. Comput Methods Appl Mech Eng 198:318–331

Luo Z, Wang MY, Wang SY, Wei P (2008b) A level set-based parameterization method for structural shape and topology optimization. Int J Numer Methods Eng 76:1–26

Luo Z, Tong LY, Kang Z (2009) A level set method for structural shape and topology optimization using radial basis functions. Comput Struct 87:425–434

Ma YS (ed.) (2013) Semantic modeling and interoperability in product and process engineering, Springer

Masmiati N, Sarhan AAD, Hamdi M (2012) Optimizing the cutting parameters for better surface quality in 2.5D cutting utilizing titanium coated carbide ball end mill. Int J Precis Eng Manuf 13:2097–2102

Mei YL, Wang XM, Cheng GD (2008) A feature-based topological optimization for structure design. Adv Eng Softw 39:71–87

Miao HK, Sridharan N, Shah JJ (2002) CAD-CAM integration using machining features. Int J Comput Integr Manuf 15:296–318

Osher S, Sethian JA (1988) Front propagating with curvature-dependent speed: algorithms based on Hamilton–Jacobi formulations. J Comput Phys 79:12–49

PareTO (2013) User manual. http://www.sciartsoft.com/files/Downloads/PareTO_User_Manual.pdf Accessed 21 July 2014

Rabbani T, van den Heuvel F (2004) Methods for fitting CSG models to point clouds and their comparison. Computer graphics and imaging, August 17–19, Kauai, Hawaii, USA

Rozvany GIN (2009) A critical review of established methods of structural topology optimization. Struct Multidiscip Optim 37:217–237

Sethian JA, Wiegmann A (2000) Structural boundary design via level set and immersed interface methods. J Comput Phys 163:489–528

Shapiro V, Tsukanov I (1999) Implicit functions with guaranteed differential properties. Fifth ACM symposium on solid modeling and applications, Ann Arbor, MI, 258–269

So BS, Jung YH, Park JW, Lee DW (2007) Five-axis machining time estimations algorithm based on machine characteristics. J Mater Process Technol 187–188:37–40

Thompson WB, Owen JC, de St. Germain HJ, Stark SR, Henderson TC (1999) Feature-based reverse engineering of mechanical parts. IEEE Trans Robot Autom 15:57–66

van Dijk NP, Maute K, Langelaar M, van Keulen F (2013) Level-set methods for structural topology optimization: a review. Struct Multidiscip Optim 48:437–472

Verma AK, Rajotia S (2008) A hint-based machining feature recognition system for 2.5D parts. Int J Prod Res 46:1515–1537

Wang MY, Wang XM (2005) A level-set based variational method for design and optimization of heterogeneous objects. Comput Aided Des 37:321–337

Wang SY, Wang MY (2006) Radial basis functions and level set method for structural topology optimization. Int J Numer Methods Eng 65: 2060–2090

Wang MY, Wang XM, Guo DM (2003) A level set method for structural topology optimization. Comput Methods Appl Mech Eng 192:227–246

Wang X, Wang MY, Guo D (2004) Structural shape and topology optimization in a level-set-based framework of region representation. Struct Multidiscip Optim 27:1–19

Wang SY, Lim KM, Khoo BC, Wang MY (2007) An extended level set method for shape and topology optimization. J Comput Phys 221: 395–421

Wang J, Gu DX, Yu ZY, Tan CB, Zhou LS (2012) A framework for 3D model reconstruction in reverse engineering. Comput Ind Eng 63: 1189–1200

Xia Q, Shi TL, Wang MY, Liu SY (2010) A level set based method for the optimization of cast part. Struct Multidiscip Optim 41:735–747

Xia L, Zhu JH, Zhang WH, Breitkopf P (2013) An implicit model for the integrated optimization of component layout and structure topology. Comput Methods Appl Mech Eng 257:87–102

Xu D, Ananthasuresh GK (2003) Freeform skeletal shape optimization of compliant mechanism. J Mech Des 125:253–261

Xu JT, Sun YW, Zhang XK (2013) A mapping-based spiral cutting strategy for pocket machining. Int J Adv Manuf Technol 67:2489–2500

Zhou MD, Wang MY (2013) Engineering feature design for level set based structural optimization. Comput Aided Des 45:1524–1537

Zuo KT, Chen LP, Zhang YQ, Yang JZ (2006) Manufacturing- and machining-based topology optimization. Int J Adv Manuf Technol 27:531–536